ISSN 1674-1056
http://cpb.iphy.ac.cn
http://iopscience.iop.org/cpb
中国物理 B
Chinese Physics
中国物理 Chinese Physics B

Spectra properties of Yb^{3+}, Er^{3+}: Sc_2SiO_5 crystal

Yanyan Xue(薛艳艳), Lihe Zheng(郑丽和), Dapeng Jiang(姜大朋), Qinglin Sai(赛青林), Liangbi Su(苏良碧), Jun Xu(徐军)

Citation: Chin. Phys. B . 2019, 28(3): 037802. **doi:** 10.1088/1674-1056/28/3/037802
Journal homepage: http://cpb.iphy.ac.cn; http://iopscience.iop.org/cpb

What follows is a list of articles you may be interested in

Increase of photoluminescence blinking frequency of 3C-SiC nanocrystals with excitation power

Zhixing Gan(甘志星), Weiping Zhou(周卫平), Ming Meng(孟明)
Chin. Phys. B . 2018, 27(12): 127804. **doi:** 10.1088/1674-1056/27/12/127804

Photodynamics of Ga_{Zn}-V_{Zn} complex defect in Ga-doped ZnO

Ai-Hua Tang(汤爱华), Zeng-Xia Mei(梅增霞), Yao-Nan Hou(侯尧楠), Xiao-Long Du(杜小龙)
Chin. Phys. B . 2018, 27(11): 117802. **doi:** 10.1088/1674-1056/27/11/117802

Crystal growth and spectral properties of Tb: Lu_2O_3

Jiaojiao Shi(施佼佼), Bin Liu(刘斌), Qingguo Wang(王庆国), Huili Tang(唐慧丽), Feng Wu(吴锋), Dongzhen Li(李东振), Hengyu Zhao(赵衡煜), Zhanshan Wang(王占山), Wen Deng(邓文), Xu Zian(徐子安), Xu Jiayue(徐家跃), Xiaodong Xu(徐晓东), Jun Xu(徐军)
Chin. Phys. B . 2018, 27(9): 097801. **doi:** 10.1088/1674-1056/27/9/097801

Crystal growth, spectroscopic characteristics, and Judd-Ofelt analysis of Dy: Lu_2O_3 for yellow laser

Jiaojiao Shi(施佼佼), Bin Liu(刘斌), Qingguo Wang(王庆国), Huili Tang(唐慧丽), Feng Wu(吴锋), Dongzhen Li(李东振), Hengyu Zhao(赵衡煜), Zhanshan Wang(王占山), Wen Deng(邓文), Xiaodong Xu(徐晓东), Jun Xu(徐军)
Chin. Phys. B . 2018, 27(7): 077802. **doi:** 10.1088/1674-1056/27/7/077802

Effects of the ion-beam voltage on the properties of the diamond-like carbon thin film prepared by ion-beam sputtering deposition

Sun Peng, Hu Ming, Zhang Feng, Ji Yi-Qin, Liu Hua-Song, Liu Dan-Dan, Leng Jian
Chin. Phys. B . 2015, 24(6): 067803. **doi:** 10.1088/1674-1056/24/6/067803

Spectra properties of Yb^{3+}, Er^{3+}: Sc_2SiO_5 crystal*

Yanyan Xue(薛艳艳)[1], Lihe Zheng(郑丽和)[2,†], Dapeng Jiang(姜大朋)[2], Qinglin Sai(赛青林)[3], Liangbi Su(苏良碧)[2], and Jun Xu(徐军)[1,4,‡]

[1] *School of Physics Science and Engineering, Institute for Advanced Study, Tongji University, Shanghai* 200092, *China*
[2] *Shanghai Institute of Ceramics, Chinese Academy of Sciences, Shanghai* 201899, *China*
[3] *Shanghai Institute of Optics and Fine Mechanics, Chinese Academy of Sciences, Shanghai* 201800, *China*
[4] *Shanghai Engineering Research Center for Sapphire Crystals, Shanghai* 201899, *China*

(Received 1 November 2018; revised manuscript received 10 January 2019; published online 23 January 2019)

The influence of Er^{3+} ions on the spectra of Yb^{3+}, Er^{3+}: Sc_2SiO_5 (SSO) single crystal, which was obtained by Czochralski (Cz) method, is discussed. The absorption coefficient at 980 nm was 13.36 cm^{-1} with a peak absorption cross-section of 1.46×10^{-20} cm^2. The emission cross-sections at 1034 nm and 1062 nm were 5.5×10^{-21} cm^2 and 4.9×10^{-21} cm^2, respectively. The fluorescence lifetime was estimated as 1.24 ms at 1061 nm. The mechanical properties of SSO single crystal were also presented.

Keywords: Yb^{3+}, Er^{3+}: Sc_2SiO_5, spectra properties, mechanical properties

PACS: 78.55.–m, 42.70.Hj, 78.45.+h **DOI:** 10.1088/1674-1056/28/3/037802

1. Introduction

High-performance InGaAs diode laser operating in the range of 900–1100 nm raises the development of Yb^{3+} doped materials for all-solid-state ultrafast laser, high power laser, and thin disk laser.[1–5] Yb^{3+} doped laser materials possess advantages over Nd^{3+} doped ones, including long radiative lifetime, small quantum defect between absorption and emission, and absence of deleterious effects such as excited state absorption, up-conversion, and concentration quenching. The combination of Er^{3+} and Yb^{3+} in up-conversion is well studied. Upon excitation at the $^4I_{11/2}$ level, the cross-relaxation process of [Er^{3+} ($^4I_{11/2} \rightarrow {}^4I_{15/2}$); Yb^{3+} ($^2F_{7/2} \rightarrow {}^2F_{5/2}$)] could occur.[6] Therefore, in this study, we choose Er^{3+} as the sensitizer in Yb^{3+} activated laser crystal.

However, the three-energy-level scheme of Yb^{3+} laser could lead to a high laser threshold due to the high thermal population of the terminal level. Quasi-four energy levels of Yb^{3+} could be introduced by selecting a crystal host with low symmetry and multi-crystallographic sites that would improve the emission band broadening and energy level splitting.[7,8] In the silicate crystal family, scandium silicate crystal (Sc_2SiO_5, SSO) possesses the low-symmetry crystal structure of monoclinic $C2/c$ space group and two non-equivalent crystallographic sites.[9–11] In addition, SSO crystal possesses high thermal conductivity ($\kappa = 7.5$ W·m^{-1}· K^{-1}) and negative thermo-optical coefficient with the dn/dT value of -6.3×10^{-6} K^{-1}.[8] With the benefits from strong coupling between ytterbium ions and crystal field, quasi-four-level Yb^{3+}: SSO single crystal exhibits large energy stark splitting of 1027 cm^{-1}, which is beneficial for generating short pulse laser[12–14] and reducing heat generated in high power laser system.[3,15,16] Li *et al.* reported a diode-pumped Yb^{3+}: SSO chirped pulse amplifier with 1 ps pulse duration.[17] SSO crystal host has been widely used in the fields of high power lasers, ultra-fast lasers, and amplifiers.

In this paper, the mechanical properties of pure Sc_2SiO_5 bulk crystal will be demonstrated for the first time. The influence of Er^{3+} ions on the near infrared spectroscopy of Yb^{3+}, Er^{3+}: SSO will also be discussed.

2. Experiments

2.1. Crystal growth

Undoped SSO crystal was grown for the measurement of fracture toughness and flexure strength. The raw materials of Sc_2O_3 (4N), SiO_2 (4N), Yb_2O_3 (4N5), and Er_2O_3 (4N5) were used for SSO and Yb^{3+}, Er^{3+}: SSO single crystals growth. The mixture powders were compressed and loaded into an alumina container before sintering at 1250 °C for 12 h in a muffle furnace. The crystals were grown by the Czochralski method in an inductively heated iridium crucible under nitrogen ambient atmosphere. SSO crystal seed oriented in (010) direction was used. The pulling rate was set at 1–2 mm/h and the rotation rate was 15–20 rpm. After pulling apart from the melting, the crystals were cooled down to room temperature

*Project supported by the National Key Research and Development Program of China (Grant No. 2016YFB0701002), the Joint Fund of the National Natural Science Foundation of China and China Academy of Engineering Physics (NSAF) (Grant No. U1530152), the National Natural Science Foundation of China (Grant Nos. 91222112 and 61475177), and Shanghai Rising-Star Program (B type), China (Grant No. 14QB1401600).

†Corresponding author. E-mail: zhenglihe@gmail.com
‡Corresponding author. E-mail: xujun@mail.shcnc.ac.cn

© 2019 Chinese Physical Society and IOP Publishing Ltd

in 40 h. SSO and Yb^{3+}, Er^{3+}: SSO crystals with diameters of 25 mm and lengths of 65 mm were obtained as shown in Fig. 1. The transparent Yb^{3+}, Er^{3+}: SSO crystal showed a light pink color.

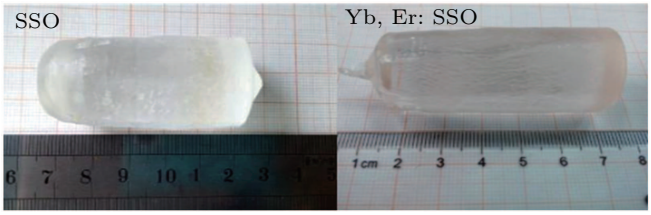


Fig. 1. Photographs of the as-grown SSO and Yb^{3+}, Er^{3+}: SSO single crystals.

2.2. Spectra measurements

The concentrations of Yb^{3+} and Er^{3+} in Yb^{3+}, Er^{3+}: SSO crystal detected by inductively coupled plasma atomic emission spectrometry (ICP-AES) were 7.07 wt.% and 0.065 wt.%, respectively. The segregation coefficient of Yb^{3+} in the Yb^{3+}, Er^{3+}: SSO crystal was calculated to be 0.85, while the segregation coefficient was 0.96 in Yb^{3+}: SSO crystal.[3] The solubility of Yb^{3+} in the Yb^{3+}, Er^{3+}: SSO host lattice was reduced due to the competition of Er^{3+} ions with Yb^{3+} while substituting in the Sc^{3+} lattice. The influence of Er^{3+} on the spectra will be further discussed in Section 3.

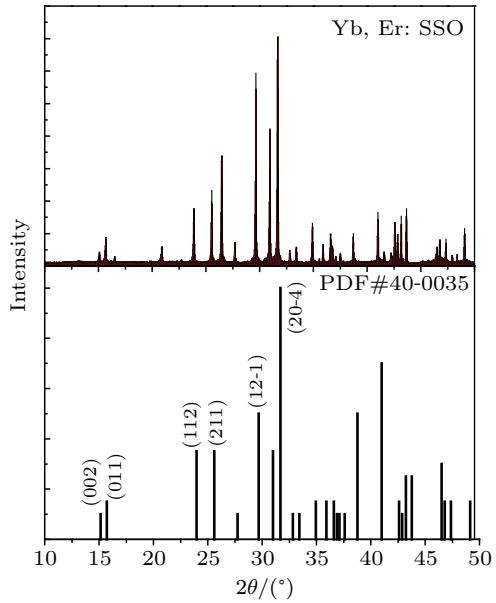


Fig. 2. XRD pattern of Yb^{3+}, Er^{3+}: SSO crystal.

Crystal structure was confirmed by x-ray diffraction (XRD, Cu target, $K\alpha$, X-pert, Holland). Figure 2 presents the x-ray powder diffraction pattern of Yb^{3+}, Er^{3+}: SSO crystal. The diffraction peak positions match well with those of standard Sc_2SiO_5 (PDF#40-0035). The XRD indicates that Yb^{3+}, Er^{3+}: SSO crystal maintains the primitive monoclinic symmetry with a space group of $C2/c$. The cell parameters were calculated to be $a = 0.9960$ nm, $b = 0.6428$ nm, $c = 1.2058$ nm, $\beta = 103.7°$ and $V = 0.7500$ nm^3. Due to a larger ionic radius of Yb^{3+} than that of Sc^{3+}, the cell volume is slightly larger than $V = 0.7498$ nm^3 of the SSO single crystal.

3. Results and discussion

3.1. Mechanical properties

To apply laser crystals in high power laser system, it is important to evaluate mechanical properties that could predict the energy storage capability of the laser host.

The Vickers hardness (H_V) and fracture toughness of SSO crystal were determined by indentation technique in a digital Vickers hardness tester (Wilson-WolpertTukon2100B) at room temperature for the first time. Mechanical properties of Nd: YAG crystal were also tested for comparison.

Figure 3 presents the image of indentation on the mechanically polished surface of the SSO crystal. The Vickers hardness can be estimated by

$$H_V = F/A, \tag{1}$$

where F is the force applied to the indenter and A is the surface area of the resulting indentation. The fracture toughness can be experimentally determined from the linear sizes of radial cracks (C) arising near the point of load application and estimated by

$$K_{Ic} = 9.81 \times 10^3 \times F\left[3.14\left(2C_1 + 2C_2\right)/4\right]^{-3/2}(\tan\beta)^{-1}, \tag{2}$$

where β is the correction angle of 68°. The flexure strength was determined by a three-point bending test on 3 mm× 5 mm× 20 mm bars which were polished after cutting using a universal testing machine (Instron-1195). Five specimens for each sample were tested.

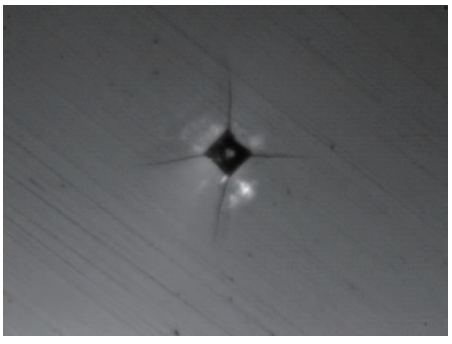


Fig. 3. Microscopic image of indentation in mechanically polished SSO crystal.

The fracture toughness and flexure strength of SSO and Nd: YAG crystals are listed in Table 1. Vickers hardnesses of SSO and Nd: YAG crystals are 908 and 1325 under the load of 0.5 kg, respectively. It can be seen that the fracture toughness of SSO is close to that of Nd: YAG crystal but higher than that of Y_2O_3 and YSO crystals. The flexure strength of SSO

is inferior to that of Y_2O_3 and Nd: YAG crystals. All obtained data indicate that the SSO crystal is suitable for mechanical processing and high power operation.

Table 1. Fracture toughness and flexure strength of SSO, Nd: YAG, and other reported crystals.

Crystal	Fracture toughness/MPa·m$^{1/2}$	Flexure strength/MPa	Ref.
Y_2O_3	0.7	150	[18]
YSO	0.54 ‖ *a*; 0.7 ‖ *b*; 0.78 ‖ *c*	–	[19]
YAG	1.0, 1.4	–	[20]
SSO	0.83	135.5	this work
Nd: YAG	0.95	301.25	this work

3.2. Absorption and emission spectra

The absorption and emission spectra at room temperature of Yb^{3+}, Er^{3+}: SSO crystal in the wavelength region of 850–1150 nm are shown in Fig. 4. The unpolarized absorption spectrum was measured by using a UV/Vis/NIR spectrophotometer (Model Cary 5000, Agilent) in the wavelength region from 400 nm to 2000 nm. The absorption spectrum is mainly composed of four strong bands around 915 nm, 958 nm, 980 nm, and 990 nm corresponding to the transitions from the ground state $^2F_{7/2}$ to the sublevels of $^2F_{5/2}$ of Yb^{3+}. The peak at 980 nm shows the highest absorption coefficient of 13.36 cm^{-1}. The absorption cross-sections of Yb^{3+} were calculated according to

$$\sigma_{\rm abs}(\lambda) = \frac{2.303 \times D_{\rm o}}{NL}, \tag{3}$$

where $D_{\rm o}$ is the optical density as a function of wavelength, N is the Yb^{3+} concentration with the value of 9.16×10^{20} ions/cm^3, and L is the sample thickness. The absorption cross-section $\sigma_{\rm abs}$ is shown in Fig. 4. The absorption cross section at 980 nm is 1.46×10^{-20} cm^2, which is larger than that of Yb^{3+}: SSO crystal.[3] It is indicated that Er^{3+} ions make contribution to the absorption intensity.

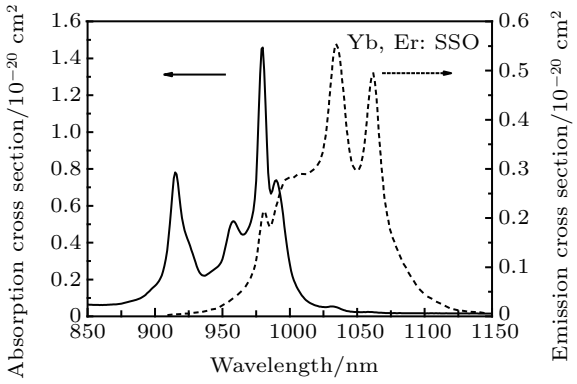


Fig. 4. The absorption and emission spectra of Yb^{3+}, Er^{3+}: SSO crystal.

The emission spectrum was investigated under the excitation of Xe lamp (Jobin-Yvon TRIAX 550 spectrophotometer) in the range of 900–1200 nm. The fluorescence spectrum is mainly composed of three bands around 998 nm, 1034 nm, and 1062 nm in addition to the zero-line at 981 nm. The fluorescence intensities at 1034 nm and 1062 nm are stronger than that at 998 nm. The shapes of absorption and fluorescence spectra are broad due to the thermal spreading of the spectra at room temperature.

A fluorescence lifetime measurement was carried out by a computer-controlled transient digitizer decay curve of emission. The fluorescence lifetime at 1061 nm was estimated to be 1.24 ms, as shown in Fig. 5. The emission cross-sections of Yb^{3+} for the transition between $^2F_{5/2}$ and $^2F_{7/2}$ can be calculated by Füchtbauer–Ladenburg formula[20]

$$\sigma_{\rm em}(\lambda) = \frac{\lambda^5 I(\lambda)}{8\pi n^2 c \tau_{\rm rad} \int \lambda I(\lambda) {\rm d}\lambda}, \tag{4}$$

where $I(\lambda)$ is the emission intensity, $\tau_{\rm rad}$ is the radiative lifetime of the excited manifold $^2F_{5/2}$ of Yb^{3+}, c is the light velocity, and n is the refractive index. The emission cross-section $\sigma_{\rm em}$ is shown in Fig. 4.

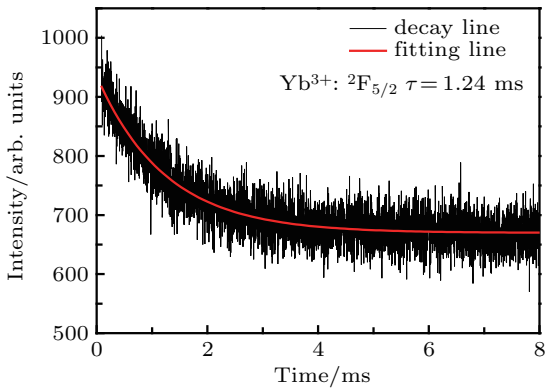


Fig. 5. The fluorescence decay curve of Yb^{3+}, Er^{3+}: SSO crystal at 1061 nm.

Table 2 shows the spectroscopic parameters of Yb^{3+}, Er^{3+}: SSO crystal. The $\sigma_{\rm abs}$ at 915 nm, 958 nm, 980 nm, and 990 nm were estimated to be 7.8×10^{-21} cm^2, 5.2×10^{-21} cm^2, 14.6×10^{-21} cm^2, and 7.4×10^{-21} cm^2, and the absorption bandwidths were around 16 nm, 19 nm, 10 nm, and 12 nm, respectively. Broad and strong absorption bands are necessary to improve the diode-pumping efficiency, because laser diodes typically emit in a 5 nm wide spectral range while presenting a thermal shift of the peak wavelength. Therefore, the absorption bands of Yb^{3+}, Er^{3+}: SSO crystal are favorable for matching the emission wavelength of InGaAs laser diodes for highly efficient pumping. Two strong fluorescence bands around 1034 nm and 1062 nm could be served as the efficient laser output with $\sigma_{\rm em}$ of 5.5×10^{-21} cm^2 and 4.9×10^{-21} cm^2, respectively. Particularly, in addition to the smallest thermal populating of the terminal laser level which brings about the smallest re-absorption losses, the emission band around 1034 nm possesses the largest emission cross-section, which is promising for low threshold and high efficient laser operation.

It should be noted that, the particularly broad emission bandwidth (FWHM) of Yb^{3+}, Er^{3+}: SSO crystal reaches 72 nm, which is broader than that of Yb: YSO (48 nm).[21]

Table 2. Spectroscopic parameters of Yb^{3+}, Er^{3+}: SSO crystal.

Parameter	Yb^{3+}, Er^{3+}: SSO	Yb^{3+}: SSO
Main absorption peak λ_{abs}/nm	980	976
Absorption cross-section $\sigma_{abs}/10^{-20}$ cm^2	1.46	0.92
Absorption bandwidth/nm	10	24
Fluorescence peak λ_{em}/nm	1034	1036
Emission cross-section $\sigma_{em}/10^{-20}$ cm^2	0.55	0.44
Emission bandwidth/nm	72	57
Fluorescence lifetime/ms	1.24	1.64

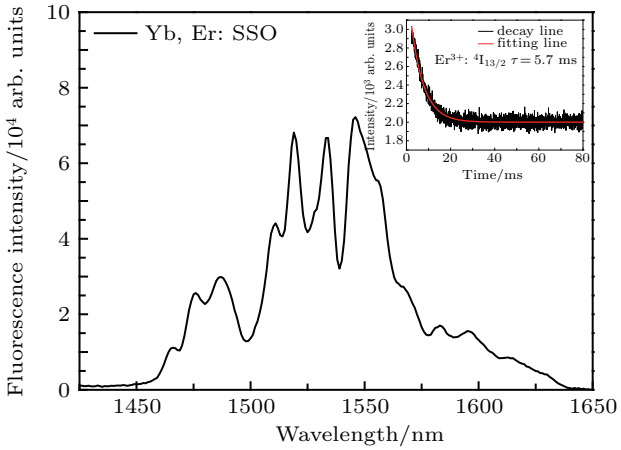


Fig. 6. The emission spectrum and fluorescence decay curve of Er^{3+} around 1548 nm.

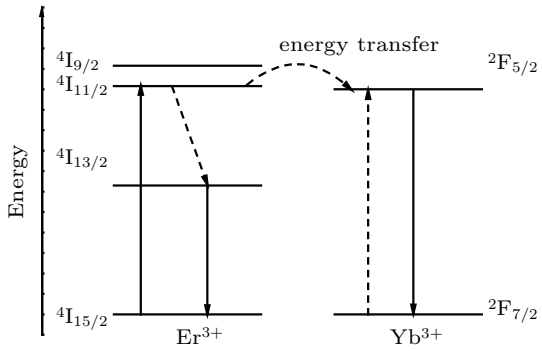


Fig. 7. Energy transfer process between Er^{3+} and Yb^{3+}.

In order to better understand the effect of Er^{3+} in Yb^{3+}, Er^{3+}: SSO crystal, the emission spectrum and fluorescence decay curve of Er^{3+} around 1548 nm are presented in Fig. 6. The fluorescence lifetime of Er^{3+} in Yb^{3+}, Er^{3+}: SSO crystal was fitted to be 5.7 ms. Energy transfer process of the Er^{3+} and Yb^{3+} in Sc_2SiO_5 host is shown in Fig. 7. The Er^{3+} in Yb^{3+}, Er^{3+}: SSO crystal could also be pumped directly to the $^4I_{11/2}$ level at the excitation wavelength of 896 nm from Xe lamp. Yb^{3+} is acceptor and the energy is transferred from the $^4I_{11/2}$ level of Er^{3+} to the $^2F_{5/2}$ level of Yb^{3+} and the cross-relaxation process of [Er^{3+} ($^4I_{11/2} \rightarrow {}^4I_{15/2}$); Yb^{3+} ($^2F_{7/2} \rightarrow {}^2F_{5/2}$)] can occur, which explains the increase of σ_{em} from 4.4×10^{-21} cm^2 in Yb^{3+}: SSO[3] to 5.5×10^{-21} cm^2 in Yb^{3+}, Er^{3+}: SSO with the co-doping of 0.065 wt.% Er^{3+}.

4. Conclusion

In summary, the fracture toughness was obtained to be 0.83 MPa·m$^{1/2}$ and flexure strength was 135.5 MPa in SSO crystal. Yb^{3+}, Er^{3+}: SSO crystal with Er^{3+} content of 0.065 wt.% shows broader emission bandwidth of 72 nm. The emission band at 1034 nm possesses the largest emission cross-section of 5.5×10^{-21} cm^2, which is favorable for low threshold and high efficient laser operation. The effective regulation of optical parameters obtained in Yb^{3+}, Er^{3+}: SSO crystal demonstrated that cations-interaction is promising in investigating new laser candidates with higher emission cross-section for high power laser systems.

References

[1] Lacovara P, Choi H K, Wang C A, Aggarwal R L and Fan T Y 1991 *Opt. Lett.* **16** 1089
[2] Tsunekane M and Taira T 2006 *Opt. Lett.* **31** 2003
[3] Zheng L H, Xu J, Zhao G J, Su L B, Wu F and Liang X Y 2008 *Appl. Phys. B* **91** 443
[4] Kim W, Baker C, Villalobos G, Frantz J, Shaw B, Lutz A, Sadowski B, Kung F, Hunt M, Sanghera J and Aggarwal I 2011 *J. Am. Ceram Soc.* **94** 3001
[5] Chen S, Wu Y Q and Yang Y 2013 *J. Am. Ceram Soc.* **96** 1694
[6] Huang X Y, Han S Y, Huang W and Liu X G 2013 *Chem. Soc. Rev.* **42** 173
[7] He J P, Liang X Y, Li J F, Zheng L H, Su L B and Xu J 2011 *Chin. Phys. Lett.* **28** 084204
[8] Tian W L, Wang Z H, Wei L, Peng Y N, Zhang J W, Zhu Z, Zhu J F, Han H N, Jia Y L, Zheng L H, Xu J and Wei Z Y 2014 *Opt. Exp.* **22** 19040
[9] Gaume R, Viana B, Derouet J and Vivien D 2003 *Opt. Mater.* **22** 107
[10] Zheng L H, Xu J, Su L B, Li H J, Ryba-Romanowski W, Lisiecki R and Solarz P 2010 *Appl. Phys. Lett.* **96** 121908
[11] Rodewald U C, Zheng L H, Heying B, Xu X D, Su L B, Xu J and Poettgen R 2012 *Z. Naturforsch. B* **67** 113
[12] Wentsch K S, Zheng L H, Xu J, Ahmed M A and Graf T 2012 *Opt. Lett.* **37** 4750
[13] Xu C W, Tang D Y, Zhang J, Zhu H Y, Xu X D, Zheng L H, Su L B and Xu J 2013 *Opt. Commun.* **294** 237
[14] Ge P G, Su L M, Liu J, Zheng L H, Su L B, Xu J and Wang Y G 2015 *Chin. Phys. B* **24** 014207
[15] Wentsch K S, Weichelt B, Zheng L H, Xu J, Ahmed M A and Graf T 2012 *Opt. Lett.* **37** 37
[16] Zhang H Y, Li J F, Liang X Y, Lin H, Zheng L H, Su L B and Xu J 2012 *Chin. Opt. Lett.* **10** 111404
[17] Li J F, Gao P, Zheng L H, Su L B, Xu J and Liang X Y 2015 *Chin. Opt. Lett.* **13** 011403
[18] Tropf W J, Thomas M E and Harris T J 1995 *Handbook of Optics* (New York: Mc Graw-Hill, Inc) pp. 33–48
[19] Weber M J 1994 *Handbook of laser science and Technology supplement 2: optical materials* (Vol. 8) (New York: CRC Press) p. 595
[20] Caird J A, Ramponi A J and Staver P R 1991 *J. Opt. Soc. Am. B* **8** 1391
[21] Yan C F, Zhao G J, Zhang L H, Xu J, Liang X Y, Du J, Li W X, Pan H F, Ding L G and Zeng H P 2006 *Solid State Commun.* **137** 451